

Aspects of using a numerical simulator for a robot position-orientation matrix determination

C O Miclosina¹ and I Halalae²

¹“Eftimie Murgu” University of Resita, Department of Mechanical Engineering and Management, Traian Vuia Square, No. 1-4, 320067 Resita, Romania

²“Eftimie Murgu” University of Resita, Department of Electrical Engineering and Informatics, Traian Vuia Square, No. 1-4, 320067 Resita, Romania

E-mail: c.miclosina@uem.ro

Abstract. The paper presents the mathematical model of a parallel topology robot of $FP_3+3\cdot RRS+MP_3$ type, used in order to determine the position-orientation matrix of the robot's mobile reference system. By using a numerical simulator, positions of the characteristic point are plotted in the 3D space.

1. Introduction

Positioning accuracy is a current requirement for the use of robots in various applications [1-4]. This could be estimated by the means of the position-orientation matrix of the reference system attached to the robot's characteristic point [5-7].

In the case of parallel topology robots, the positioning of the end effector is more complex than in the case of serial topology robots [8-11]. Different structures of parallel topology robots were analyzed in [12-16].

The paper proposes a certain structure of a parallel topology robot and a manner of position-orientation matrix determination by using a numerical simulator.

2. The Kinematical Scheme of the Guiding Device Mechanism

The structure of the guiding device mechanism with parallel topology is $FP_3+3\cdot RRS+MP_3$ [2], [5], [6]. It contains 2 platforms, a fixed one (FP_3), and a mobile one (MP_3), linked by 3 identical open kinematical chains RRS. Every open kinematical chain, or “connexion”, contains 2 binary links, 1 driving rotational joint (R), 1 rotational joint (R) and 1 spherical joint (S).

The concept „connexion” was introduced in Mechanism Theory and Robotics by Professor F.V. Kovacs. According to [17], [18], a ”connexion” is an open linkage interposed between two links, aiming the change of the number of their relative degrees of freedom (DOF).

The kinematical scheme of the guiding device mechanism with parallel topology is presented in Figure 1 [2], [5], [6].

The driving rotational joints are A_1 , A_2 and A_3 .



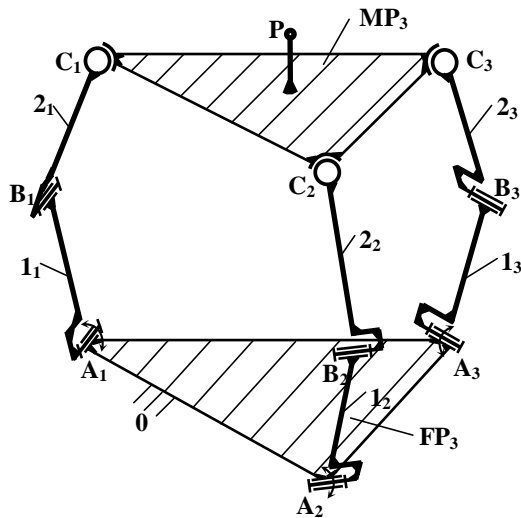


Figure 1. The kinematical scheme of the guiding device mechanism of $FP_3+3 \cdot RRS+MP_3$ type [2], [5], [6]

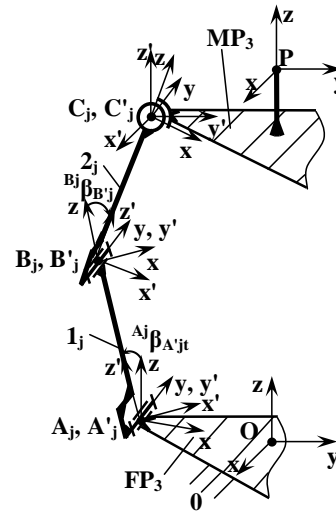


Figure 2. The frames attached to the links of the connexion $A_jB_jC_j$ [5], [6]

The links dimensions are as follows [2], [5], [6]:

- the fixed platform: equilateral triangle with the sides $\overline{A_1A_2} = \overline{A_2A_3} = \overline{A_3A_1} = 125$ [mm] ;
- the mobile platform: equilateral triangle with the sides $\overline{C_1C_2} = \overline{C_2C_3} = \overline{C_3C_1} = 125$ [mm] ;
- lengths of links 1₁, 1₂, and 1₃: $\overline{A_1B_1} = \overline{A_2B_2} = \overline{A_3B_3} = 60$ [mm] ;
- lengths of links 2₁, 2₂, and 2₃: $\overline{B_1C_1} = \overline{B_2C_2} = \overline{B_3C_3} = 95$ [mm] ;
- the distance from point P to plane $C_1C_2C_3$ is 35,7 [mm].

The points A_j, B_j, C_j ($j = 1, 2, 3$) were considered in the geometrical centers of the kinematical joints.

3. Mathematical Modeling of the Mechanism

The mathematical modeling was developed in previous work [5], [6], by using the “Pair of Frames” (PF) concept, defined by Professor F.V. Kovacs in [19], as well as its using for modeling of mechanical systems. Generalized joints and generalized offsets can be mathematically modeled by means of transformation matrices between 3D (or 2D) frames, attached in the first case to each of the links constituting the generalized offset [19].

Figure 2 presents the frames attached to the links of the connexion $A_jB_jC_j$ ($j = 1, 2, 3$) from Figure 1 [5], [6].

The frames are referred by means of their origins.

Thus, the origins of the frames attached on the links of the rotational joint A_j are placed in the geometrical center of joint A_j , and in the point O, chosen on the fixed platform FP_3 . The frames origins O and A_j belong to FP_3 and A'_j belongs to link 1_j. So, the rotational joint A_j is modelled by the $A_j-A'_j$ pair of frames; the relative rotational displacement is executed around A_jy axis with an angle ${}^{A_j}\beta_{A'_j,t}$ at the considered moment of time t [5], [6].

The origins of the frames attached on the links of the rotational joint B_j are chosen in the geometrical center of joint B_j , one on the link 1_j (B_j), and the other on the link 2_j (B'_j). The rotational joint B_j is modelled by the $B_j-B'_j$ pair of frames; the relative rotational displacement is executed around B_jy axis with an angle ${}^{B_j}\beta_{B'_j}$ [5], [6].

The origins of the frames attached to the spherical joint C_j are chosen one on the link 2_j (C_j) and the other on the mobile platform MP_3 (C'_j). The points C_j and C'_j are placed in the geometrical center of the spherical joint. The spherical joint C_j is modeled by the C_j - C'_j pair of frames. The 3D rotation is composed by a rotation around C_{jx} axis with an angle ${}^{C_j}\alpha_{C'_j}$, a rotation around C_{jy} axis with an angle ${}^{C_j}\beta_{C'_j}$ and a rotation around C_{jz} axis with an angle ${}^{C_j}\gamma_{C'_j}$ [5], [6].

In order to simplify the computation, A_{jy} , A'_{jy} , B_{jy} , B'_{jy} and C_{jy} axes are chosen parallel [5], [6].

The position-orientation matrix of mobile reference system attached to the characteristic point P can be written [5], [6]:

$${}^{FP_3}S_{MP_3} = \begin{bmatrix} n_{Px} & o_{Px} & a_{Px} & p_x \\ n_{Py} & o_{Py} & a_{Py} & p_y \\ n_{Pz} & o_{Pz} & a_{Pz} & p_z \\ 0 & 0 & 0 & 1 \end{bmatrix} = {}^O\underline{T}_P = {}^O\underline{T}_{A_j} \cdot {}^{A_j}\underline{T}_{A'_j} \cdot {}^{A'_j}\underline{T}_{B_j} \cdot {}^{B_j}\underline{T}_{B'_j} \cdot {}^{B'_j}\underline{T}_{C_j} \cdot {}^{C_j}\underline{T}_{C'_j} \cdot {}^{C'_j}\underline{T}_P = \left(\prod_j^P \underline{T} \right)_j \quad (1)$$

The matrix elements n_{Px} , o_{Px} , a_{Px} , n_{Py} , o_{Py} , a_{Py} , n_{Pz} , o_{Pz} , a_{Pz} are the projections of the \bar{n}_p , \bar{o}_p , \bar{a}_p unit vectors of the $Pxyz$ reference system on the Ox , Oy , Oz axes. The elements p_x , p_y , p_z are the projections of the \overline{OP} position vector of the P point on the $Oxyz$ reference system axes [5], [6].

The position-orientation matrix of the characteristic point P is identical for every connexion 1, 2, and 3. Following, 3 relations of type (1) can be equalized, as shown in equation system (2) [5], [6].

$$\begin{cases} \left(\prod_j^P \underline{T} \right)_1 = \left(\prod_j^P \underline{T} \right)_2 \\ \left(\prod_j^P \underline{T} \right)_2 = \left(\prod_j^P \underline{T} \right)_3 \\ \left(\prod_j^P \underline{T} \right)_1 = \left(\prod_j^P \underline{T} \right)_3 \end{cases} \quad (2)$$

In scalar form, for $j = 1, 2, 3$, by equalizing the elements of matrixes in expression (2), it can be obtained a scalar equation system with $4 \cdot 4 \cdot 3 = 48$ equations [5], [6].

Considering that the equalization of position-orientation matrixes for the connexions 1 and 3 leads to redundant equations, and the equalization of the last line of the matrixes leads also to redundant equations, the number of equations which can be used to solving the system is $4 \cdot 4 \cdot 2 - 2 \cdot 4 = 24$ [5], [6].

The parameters ${}^{A_j}\beta_{A'_j}$ ($j = 1, 2, 3$) at the time t are known. From equation system (2), 12 elements with different values of 0 and 1 of the position - orientation matrix ${}^{FP_3}S_{MP_3}$ can be computed. The variable angles ${}^{B_j}\beta_{B'_j}$, ${}^{C_j}\alpha_{C'_j}$, ${}^{C_j}\beta_{C'_j}$ and ${}^{C_j}\gamma_{C'_j}$ (for $j = 1, 2, 3$), totally 12 angles, are unknown. This means that $24 - 12 = 12$ scalar equations of system (5) are redundant [5], [6].

For the connexion 1, $j = 1$ and the matrixes from relation (1) are as follows [5], [6]:

$${}^O\underline{T}_{A_1} = \text{Transl}\left[x, (l_{OA_1})_x\right] \cdot \text{Transl}\left[y, (l_{OA_1})_y\right] \cdot \text{Rot}\left(z, O\hat{A}_1A_2\right) = \begin{bmatrix} \cos O\hat{A}_1A_2 & -\sin O\hat{A}_1A_2 & 0 & (l_{OA_1})_x \\ \sin O\hat{A}_1A_2 & \cos O\hat{A}_1A_2 & 0 & (l_{OA_1})_y \\ 0 & 0 & 1 & 0 \\ 0 & 0 & 0 & 1 \end{bmatrix}; \quad (3)$$

$${}^{A_1}\underline{T}_{A_1} = Rot(y, {}^{A_1}\beta_{A_1t}) = \begin{bmatrix} \cos {}^{A_1}\beta_{A_1t} & 0 & \sin {}^{A_1}\beta_{A_1t} & 0 \\ 0 & 1 & 0 & 0 \\ -\sin {}^{A_1}\beta_{A_1t} & 0 & \cos {}^{A_1}\beta_{A_1t} & 0 \\ 0 & 0 & 0 & 1 \end{bmatrix}; \quad (4)$$

$${}^{A_1}\underline{T}_{B_1} = Transl[z, (l_{A_1B_1})_z] = \begin{bmatrix} 1 & 0 & 0 & 0 \\ 0 & 1 & 0 & 0 \\ 0 & 0 & 1 & (l_{A_1B_1})_z \\ 0 & 0 & 0 & 1 \end{bmatrix}; \quad (5)$$

$${}^{B_1}\underline{T}_{B_1} = Rot(y, {}^{B_1}\beta_{B_1}) = \begin{bmatrix} \cos {}^{B_1}\beta_{B_1} & 0 & \sin {}^{B_1}\beta_{B_1} & 0 \\ 0 & 1 & 0 & 0 \\ -\sin {}^{B_1}\beta_{B_1} & 0 & \cos {}^{B_1}\beta_{B_1} & 0 \\ 0 & 0 & 0 & 1 \end{bmatrix}; \quad (6)$$

$${}^{B_1}\underline{T}_{C_1} = Transl[z, (l_{B_1C_1})_z] = \begin{bmatrix} 1 & 0 & 0 & 0 \\ 0 & 1 & 0 & 0 \\ 0 & 0 & 1 & (l_{B_1C_1})_z \\ 0 & 0 & 0 & 1 \end{bmatrix}; \quad (7)$$

$$\begin{aligned} {}^{C_1}\underline{T}_{C_1} &= Rot(x, {}^{C_1}\alpha_{C_1}) \cdot Rot(y, {}^{C_1}\beta_{C_1}) \cdot Rot(z, {}^{C_1}\gamma_{C_1}) = \\ &= \begin{bmatrix} 1 & 0 & 0 & 0 \\ 0 & \cos({}^{C_1}\alpha_{C_1}) & -\sin({}^{C_1}\alpha_{C_1}) & 0 \\ 0 & \sin({}^{C_1}\alpha_{C_1}) & \cos({}^{C_1}\alpha_{C_1}) & 0 \\ 0 & 0 & 0 & 1 \end{bmatrix} \cdot \begin{bmatrix} \cos({}^{C_1}\beta_{C_1}) & 0 & \sin({}^{C_1}\beta_{C_1}) & 0 \\ 0 & 1 & 0 & 0 \\ -\sin({}^{C_1}\beta_{C_1}) & 0 & \cos({}^{C_1}\beta_{C_1}) & 0 \\ 0 & 0 & 0 & 1 \end{bmatrix} \cdot \begin{bmatrix} \cos({}^{C_1}\gamma_{C_1}) & -\sin({}^{C_1}\gamma_{C_1}) & 0 & 0 \\ \sin({}^{C_1}\gamma_{C_1}) & \cos({}^{C_1}\gamma_{C_1}) & 0 & 0 \\ 0 & 0 & 1 & 0 \\ 0 & 0 & 0 & 1 \end{bmatrix}; \quad (8) \end{aligned}$$

$$\begin{aligned} {}^{C_1}\underline{T}_P &= Transl[x, (l_{C_1P})_x] \cdot Transl[y, (l_{C_1P})_y] \cdot Transl[z, (l_{C_1P})_z] = \\ &= \begin{bmatrix} 1 & 0 & 0 & (l_{C_1P})_x \\ 0 & 1 & 0 & 0 \\ 0 & 0 & 1 & 0 \\ 0 & 0 & 0 & 1 \end{bmatrix} \cdot \begin{bmatrix} 1 & 0 & 0 & 0 \\ 0 & 1 & 0 & (l_{C_1P})_y \\ 0 & 0 & 1 & 0 \\ 0 & 0 & 0 & 1 \end{bmatrix} \cdot \begin{bmatrix} 1 & 0 & 0 & 0 \\ 0 & 1 & 0 & 0 \\ 0 & 0 & 1 & (l_{C_1P})_z \\ 0 & 0 & 0 & 1 \end{bmatrix}, \quad (9) \end{aligned}$$

where $(l_{OA_j})_x$, $(l_{OA_j})_y$, etc., are the projections of the segments $\overline{OA_j}$, etc., on the axes Ox, Oy (for $j = 1, 2, 3$) [5], [6].

For the connexions 2 and 3, the matrixes from relation (1) can be written in a similar manner, as presented in [5], [6].

4. Scilab Numerical Simulator

Scilab, a free and open source software [20], was used for numerical calculus and plotting results.

For example, for the input parameters ${}^{A_1}\beta_{A_1} = 90[^\circ]$; ${}^{A_2}\beta_{A_2} = 90[^\circ]$; ${}^{A_3}\beta_{A_3} = 90[^\circ]$, the characteristic point P has the coordinates $p_x = 0[\text{mm}]$; $p_y = 0[\text{mm}]$; $p_z = 109,355 [\text{mm}]$; for the input parameters ${}^{A_1}\beta_{A_1t} = 0[^\circ]$; ${}^{A_2}\beta_{A_2t} = 0[^\circ]$; ${}^{A_3}\beta_{A_3t} = 0[^\circ]$, the coordinates of the characteristic point P are

$p_x = 0$ [mm]; $p_y = 0$ [mm]; $p_z = 190,700$ [mm]. These points and the trajectory of the characteristic point between them, obtained with Scilab software, are presented in Figure 3.

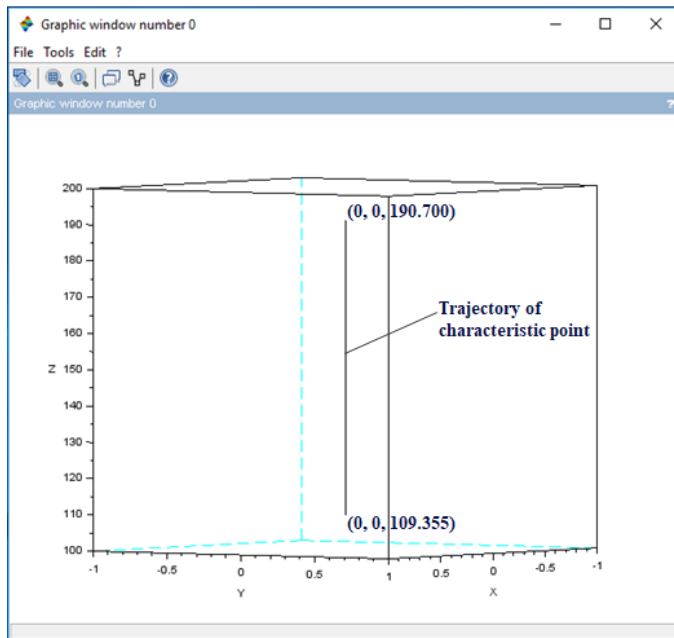


Figure 3. Vertical trajectory of the characteristic point P from the minimum position (0, 0, 109,355) to the maximum position (0, 0, 190,700) on z axis.

Figure 4 shows the trajectory of the characteristic point P from position defined by coordinates (-11.620, -6.709, 152.834) to position (4.066, 2.347, 181.492), for the input parameters ${}^{A_1} \beta_{A_1,t} = 90$ [°]; ${}^{A_2} \beta_{A_2,t} = 30,6$ [°]; ${}^{A_3} \beta_{A_3,t} = 30,6$ [°] and ${}^{A_1} \beta_{A_1,t} = 0$ [°]; ${}^{A_2} \beta_{A_2,t} = 30,6$ [°]; ${}^{A_3} \beta_{A_3,t} = 30,6$ [°] respectively.

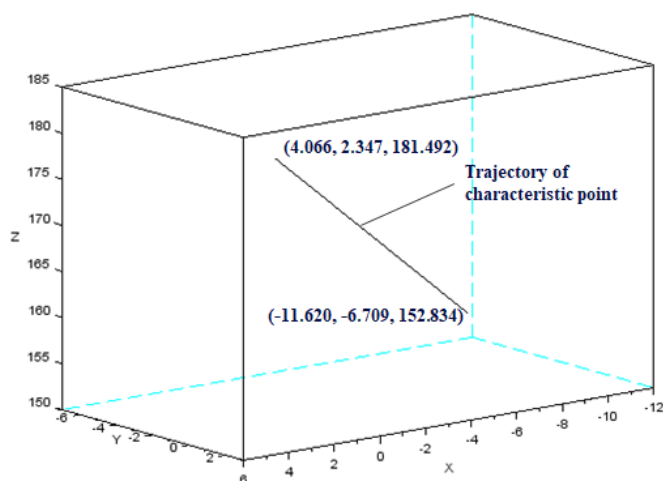


Figure 4. Trajectory of the characteristic point P from position (-11.620, -6.709, 152.834) to position (4.066, 2.347, 181.492).

5. Conclusions

By using the SciLab software, the calculus for determination of position-orientation matrix of a certain parallel topology robot structure is performed. This is a part of more complex project regarding the numerical simulation of mechanisms.

The trajectory of the characteristic point can be accomplished for different input parameters.

As further research, this manner of numerical calculus can be applied to other parallel topology mechanism structures.

References

- [1] Merlet J P 2006 *Parallel Robots*, 2nd ed., Springer, Dordrecht, Nederland
- [2] Miclosina C O 2009 *Roboti industriali si linii flexibile / Industrial Robots and Flexible Lines*, Eftimie Murgu Publishing House, Resita, Romania
- [3] Tian H, Wang C, Dang X and Sun L 2017 A 6-DOF parallel bone-grinding robot for cervical disc replacement surgery, *Medical & Biological Engineering & Computing* **55**(12) 2017-2121
- [4] Anderson P L, Mahoney A W and Webster R J III 2017 Continuum reconfigurable parallel robots for surgery: shape sensing and state estimation with uncertainty, *IEEE Robotics and Automation Letters* **2**(3) 1617-1624
- [5] Miclosina C O 2005 Geometrical Modelling of a $FP_3+3\times RRS+MP_3$ Type Parallel Robotic Guiding Device, Using the „Connexion” and „Pair of Frames” Concepts, *Robotica & Management* **10**(2) 72-76
- [6] Miclosina C 2006 *Contributii la analiza si sinteza mecanismelor robotilor cu topologie paralela, utilizand notiunea de “conexiune” / Contributions to the Analysis and Synthesis of Parallel Topology Robots Mechanisms, Using the Notion of „Connexion”*, Politehnica University of Timisoara, Doctoral Thesis
- [7] Miclosina C O 2009 Six inextensible wire device for determination of position-orientation matrix of a robot's mobile reference system, *Annals of DAAAM for 2009 & Proc. of the 20th Int. DAAAM Symp. (Vienna)* 841-842
- [8] Martini A 2018 Gravity compensation of a 6-UPS parallel kinematics machine tool through elastically balanced constant-force generators, *FME Transactions* **46**(1) 10-16
- [9] Acevedo M, Ceccarelli M and Carbone G 2012 Application of counter-rotary counterweights to the dynamic balancing of a spatial parallel manipulator, *Applied Mechanics and Materials* **162** 224-233
- [10] Moldovan C and Dolga V 2008 Parallel robot with variable link length mechanisms, *Annals of DAAAM for 2008 & Proceedings of the 19th Int. DAAAM Symp.(Trnava)* 897-898
- [11] Moghadam A A A, Kouzani A, Torabi K, Kaynak A and Shahinpoor M 2015 Development of a novel soft parallel robot equipped with polymeric artificial muscles, *Smart Mater. Struct.* **24** 035017
- [12] Chunikhin A Y and Glazunov V A 2017 Developing the mechanisms of parallel structure with five degrees of freedom designed for technological robots, *Journal of Machinery Manufacture and Reliability* **46**(4) 313-321
- [13] Miclosina C O, Cojocaru V and Korca Z I 2015 Dynamic simulation of a parallel topology robot operation, *Applied Mechanics and Materials* **762** 107-112
- [14] Rat N R, Neagoe M, Diaconescu D and Stan S D 2011 Dynamic analysis of a Triglidge parallel robot, *4th Int. Conf. on Human System Interaction (HIS 2011) (Yokohama)* 245-249
- [15] Ociepka P and Herbus K 2015 Strength analysis of parallel robot components in PLM Siemens NX 8.5 program, *IOP Conf. Ser.: Mater. Sci. Eng.* **95** 012101
- [16] Miclosina C O and Campian C V 2012 Fatigue analysis of low level links of a parallel topology robot guiding device mechanism, *Applied Mechanics and Materials* **162** 98-105
- [17] Kovacs F V, Perju D and Savii G 1976 *Metode noi în sinteza mecanismelor / New Methods in Mechanisms Synthesis*, Facla Publishing House, Timisoara
- [18] Kovacs F V 1997 *Using the concept ‘connexion’ for structural analysis/synthesis of parallel topology robots*, The Seventh IFToMM International Symposium on Linkages and CAD Methods, Bucharest, Romania, Vol. 2, pp 189-194
- [19] Kovacs F V 2001 Notiunea “Perechi de Sisteme de Referință” (PeSiR) și unele utilizări în domeniul de știință tehnică / The Notion “Pair of Frames” (PF) and Some Uses in Technical Science Fields, *Robotica & Management* **6**(1) 22-29
- [20] ***www.scilab.org